https://doi.org/10.30799/jnst.S105.26110205 J. Nanosci. Tech. - Volume 11 Issue 2 (2026) 1058–1061

Share Your Innovations through JACS Directory

Journal of Nanoscience and Technology

Visit Journal at https://www.jacsdirectory.com/jnst

ISSN: 2455-0191

Structural, Microstructural, and Electrical Properties of Pyrolyzed SnO_2–ZnO Nanocomposite Thin Films

Pratik H. Naik*

Nanomaterial's Research Lab., Department of Physics, Shri. Vitthalrao Shankarrao Naik A.C.S. College, Raver – 425 508, Maharashtra, India.

ARTICLEDETAILS

Article history:
Received 27 January 2026
Accepted 16 February 2026
Available online 08 March 2026

Keywords:
TEP
Spray Pyrolysis
Nanocomposites
SnO_2-ZnO Thin Film

ABSTRACT

Films of SnO_2-ZnO nano composites were produced by spray pyrolysis (SP) on a glass substrate that had been heated to 250 °C. Utilising a solution mixture of AR grade zinc acetate dehydrate and tin chloride dehydrate in deionised water with varying concentrations of tin chloride dehydrate (while maintaining a concentration of 0.05 M for zinc acetate dihydrate), the effect of thickness on structural, microstructural, and electrical properties on thin films was investigated. In order to determine the crystal structure, surface morphology, microstructural properties, and elemental composition of the produced thin films, various analytical techniques, including XRD, SEM, TEM, and EDAX, were used. Thickness of deposited SnO_2-ZnO films was calculated and found to be 190 nm, 231 nm and 361 nm with respect to the samples S1, S2 and S3. As the thickness increases, the FWHM value goes down and texture coefficient (TC) goes up which means that the films are more crystalline. The grain size was found to be between 29 and 35 nm. TEM images show that the average grains are nanocrystalline. The SnO_2-ZnO nanocomposites films were seen to be the n-type material. Average grain size and texture coefficients were found to rise with film thickness, while micro stain, standard deviation, and activation energy values decreased. The findings are examined and analysed.

1. Introduction

Nowadays, there is a lot of interest in using different self-organising processes to create metal oxide thin films on surfaces as nanocomposites. These materials are employed in molecular electronics and sensors. These nanocomposites have unique optical, chemical, mechanical, and electrical characteristics [1].

The energy band gaps of ZnO and SnO_2 are 3.4 and 3.6 eV, respectively, making them broad direct band gap semiconductors [2]. The recombination of electron-hole couples is also shown to be effectively slowed by differences in their band gap widths. In applications involving solar cells, this characteristic subsequently boosts photo catalytic activity [3]. In order to couple and produce ZnO and SnO_2 nanocomposites, numerous researchers used a variety of synthesis techniques, such as ball milling, micro emulsion, partial solid-state reduction, and co-precipitation [4,5] and thus garnered a lot of interest. Because of their extensive use in photoluminescence, transparent semiconductors, photo catalysts, piezoelectricity, gas sensors, UV light emitting devices, varistors, and optical devices, ZnO thin films are significant materials [6-10].

Tetragonal in structure, SnO_2 is an n-type semiconductor [11-14]. Among the most promising materials for gas sensors is this one. Nonetheless, the manufacture of semiconductor gas sensors directly affects their physical and sensing features, such as particle size, sensing film shape, and film thickness [15-20].

In this work, spray pyrolysis was used to create SnO_2-ZnO nanocomposites films. Microstructural properties, surface morphology, and crystal structure were investigated using transmission electron microscopy (TEM), scanning electron microscopy (SEM), and X-ray diffractogram (XRD). Utilising an energy dispersive spectrophotometer (EDAX), the composition of the elements was examined. Using two probes, electrical conductivity is measured. To identify the type of material, thermoelectric power setup (TEP) is utilised.

2. Experimental Methods

The spray pyrolysis method for creating SnO_2-ZnO nanocomposites films is depicted in Fig. 1. The spraying chamber, spray nozzle (gun), carrier gas compressor, heating system and temperature indication make up the setup.

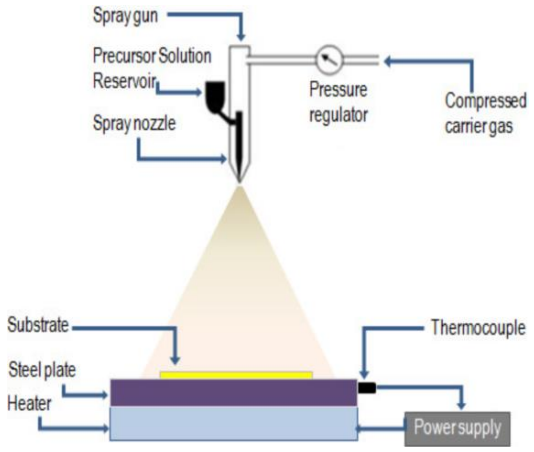

Fig. 1 System of spray pyrolysis

Zinc acetate dihydrate ($Zn(CH_3COO)_2.2H_2O$) and tin chloride dehydrate ($SnCl_2.2H_2O$) were sprayed as a starting material to create SnO_2-ZnO nanocomposite films. AR grade zinc acetate dihydrate and tin chloride dehydrate solution mixed in deionised water with varying concentrations of tin chloride dehydrate (0.025, 0.050, and 0.075 M) while maintaining the concentration of zinc acetate dihydrate (0.05 M). In order to prepare SnO_2-ZnO thin films, a few droplets of hydrochloric acid (HCl) were added. As a result, homogenous and well-adherent SnO_2-ZnO nanocomposite thin films were formed. Details about the creation of SnO_2-ZnO nanocomposites are provided elsewhere [21]. The obtained SnO_2-ZnO nanocomposites film samples were annealed at 550 °C for one hour and were designated as samples S1, S2, and S3, respectively. The concentrations of solutions needed to create SnO_2-ZnO nanocomposites films are listed in Table 1.

*Corresponding Author:pratiknaik818@gmail.com(Pratik H. Naik)

https://doi.org/10.30799/jnst.S105.26110205

Table 1 Concentration and reactant amounts of spraying solutions

Sample ID	Concentration of Zn $(CH_3COO)_2.2H_2O$ (M)	Concentration of $SnCl_2.2H_2O$ (M)	Reactants
S1	0.025	0.050	SnO_2:ZnO
S2	0.050	0.050	SnO_2:ZnO
S3	0.075	0.050	SnO_2:ZnO

3. Results and Discussion

3.1 Thickness Thin Film Measurement

A micro gravimetrical approach [22] was used to quantify the film thickness while taking the bulk zinc oxide and tin oxide densities into account. The films were placed on sanitised glass slides whose mass had already been established. The amount of deposited SnO_2-ZnO was determined by weighing the substrate once again after the deposition. Thickness was calculated and found to be 190 nm, 231 nm and 361 nm with respect to the samples S1, S2 and S3 using the following relation by measuring the deposited film's surface area while accounting for its specific weight, $T= M_{SnO2\text{-}ZnO} /A*w *10^4$, where, A is the surface area of the film [cm^2], $M_{SnO2\text{-}ZnO}$ is the quantity of the deposited tin oxide zinc oxide and w is the specific weight of SnO_2-ZnO.

3.2 Properties of Structures

3.2.1 X-Ray Diffraction Study

In order to understand the structural, microstructural, and electrical characteristics of SnO_2-ZnO nanocomposite films, structural characterisation is crucial. The X-ray diffractogram of SnO_2-ZnO nanocomposite films are displayed in Figs. 2(a-c) which were obtained between 2θ values of 20 and 80 degrees.

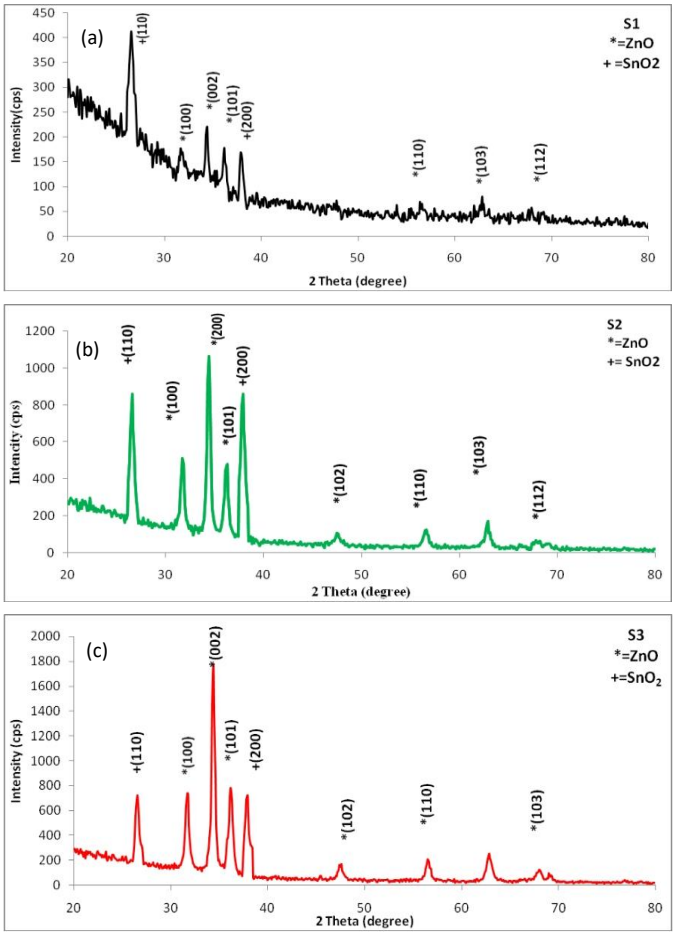

Fig. 2 X-ray diffraction patterns SnO_2-ZnO nanocomposites S1-S3.

All of the films were nanocrystalline in nature with a mixed phase of tetragonal (SnO_2) and hexagonal (ZnO), according to the XRD data. As the layer thickness increases, plane's intensity (002) also increases. It is caused by an increase in film thickness rather than structural alterations in the films [23]. SnO_2 diffraction peaks (+): (110), (200) match standard JCPDS data (Card No.05-0467) of SnO_2, while ZnO diffraction peaks (*): (100), (002), (102), (110), (103) match standard JCPDS data (Card No. 36-1491) of ZnO. Using Scherer's formula [1], the samples' average crystallite sizes were determined to be 27-33 nm, respectively, showing their nanocrystalline nature.

Table 2 displays the XRD parameters recorded for samples S1, S2, and S3, including 'd' values, full width at half maximum values of the films, and average grain size, reflecting the compositional variation of Sn in ZnO (S1 to S3). As the thickness increases, the FWHM value goes down, which means that the films are more crystalline [24]. Fig. 2 also shows that the amount of crystallinity goes up from S1 to S3. This means that the sample (S3) gets more crystalline as it gets higher. Table 4 shows that the average grain size gets bigger as the thickness gets bigger.

Table 2 XRD parameters recorded for samples S1, S2, and S3

hkl	2θ	d values			FWHM			Grain size		
plane	degree	S1	S2	S3	S1	S2	S3	S1	S2	S3
110	26.59	3.3242	3.3241	3.3240	1.123	1.100	0.996	17	19	21
100	31.79	2.6112	2.6211	2.6210	0.665	0.660	0.656	28	30	34
002	34.46	2.4015	2.4013	2.4012	1.442	1.439	1.437	16	19	36
101	36.29	1.7905	1.7904	1.7903	0.567	0.561	0.557	29	32	34
200	37.96	1.505	1.504	1.503	1.342	1.340	1.336	18	21	24
110	56.62	1.2106	1.2104	1.2101	0.421	0.417	0.413	31	33	36
103	62.88	1.1239	1.1236	1.1232	0.312	0.310	0.307	34	37	39
112	67.98	0.569	0.567	0.560	0.289	0.286	0.265	36	37	39

3.2.2 Texture Coefficient and Standard Deviation for Thin Films of SnO_2-ZnO Nanocomposite

Table 3 displays the texture coefficient (TC) of SnO_2-ZnO nanocomposite films. As the thickness of the film increases for samples S1, S2, and S3, the texture coefficient (TC) for different planes keeps going up, but the standard deviation value keeps going down, as shown in Table 3. The formula for the texture coefficient (TC) and standard deviation is used as per Moholkar et al. [25]. One possible reason for this is that as the concentration of the solution goes up, more Sn is added to the film.

Table 3 shows the texture coefficient and standard deviation for samples S1-S3

hkl	Texture coefficient			Standard deviation		
plane	S1	S2	S3	S1	S2	S3
110	1.44	1.71	1.97	10.22	10.09	9.66
100	0.87	0.916	1.03	8.6	8.45	8.36
002	2.71	2.78	2.83	9.65	9.56	9.40
101	1.10	1.22	1.61	7.66	7.52	7.45
200	1.53	1.60	1.70	9.71	9.68	9.54
110	0.47	0.50	0.53	5.69	5.63	5.49
103	0.57	0.62	0.66	4.13	3.90	3.86
112	0.23	0.27	0.29	5.26	5.12	5.09

3.2.3 Microstructural Specifics and Examination for SnO_2-ZnO Nanocomposites Thin Film

The main reasons for the broadening of X-ray diffraction line profiles are the instrument's non-ideal optics, wavelength dispersion, and microstructural flaws in the crystals. Microstructural line broadening can be categorised into size broadening and strain broadening. Size broadening happens because domains are surrounded by stacking faults, twins, or other flaws that diffract incoherently with each other. Strain broadening occurs due to a fluctuating displacement of atoms relative to their reference lattice positions. The SnO_2-ZnO thin film that was made up of nanocrystals. On the other hand, lattice strain broadening happens when the displacement changes cause the peaks of X-ray diffraction lines to shift [26]. Non-uniform tensile and compression strain, on the other hand, causes diffraction lines to broaden (microstrain). So, the effects of grain size and microstrain are linked in the way that peaks broaden, which makes it hard to tell them apart. The Williamson–Hall method assumes that both grain-size and microstrain-broadened profiles are Lorentzian [27, 28]. From this premise, a mathematical correlation was formulated between the integral breadth (β) and the volume of the weighted average grain size (D) as specified in the equation,

$$\beta\cos\theta/\lambda = 1/D + \varepsilon(\sin\theta/\lambda)$$

where, β = full width at half maxima of peak measured in radian; θ = diffraction angle; λ = wavelength of X-ray; D = grain size and ε = microstrain.

The slope of the plot between β cos θ/λ and sin θ/λ shows microstrain, and the inverse of the intercept of the y-axis shows grain size. The Williamson-Hall plot of SnO_2-ZnO nanocomposites [29] thin films made from different concentrations of Sn solution in ZnO is shown in Fig. 3. It was shown that as the concentration of the Sn precursor solution

https://doi.org/10.30799/jnst.S105.26110205

increases, the grain size rises from 27 nm to 33 nm. As the films get thicker, the microstrain values go down, which means that the microstrain in the film is tensile (Fig. 4). It goes down as the thickness of the films goes up, which means that thicker films are more relaxed. This means that films that are thicker have better crystallinity [24].

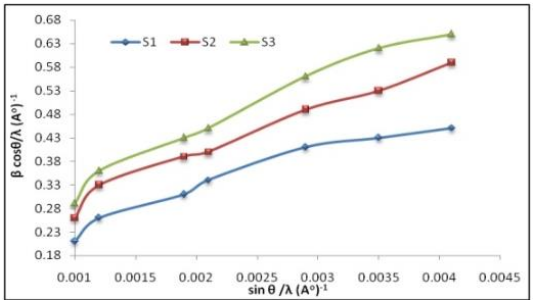

Fig. 3 Variation of βcosθ/λ with sinθ/λ

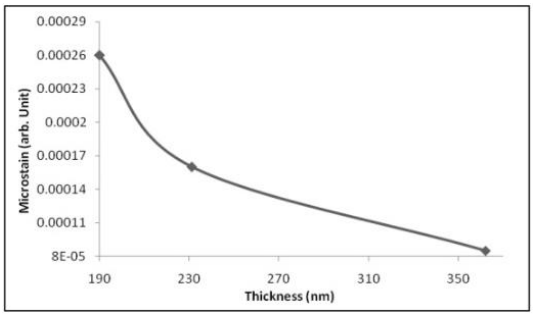

Fig. 4 Change in microstrain with film thickness

3.3 Study of Microstructure

3.3.1 Scanning Electron Microscope (SEM)

Fig. 5 shows SEM images of SnO_2-ZnO nanocomposites. The scanning electron microscope can see nanoparticles in the film even when it is magnified to "30E+3." Figs. 5(a-c) illustrate the spherical morphology of the particles in the SnO_2-ZnO nanocomposite thin film. In Fig. 5(c), a mix of spherical and cubic grains are seen, which indicates that SnO_2-ZnO nanocomposites thin film is forming. The grain size was found to be between 29 and 35 nm.

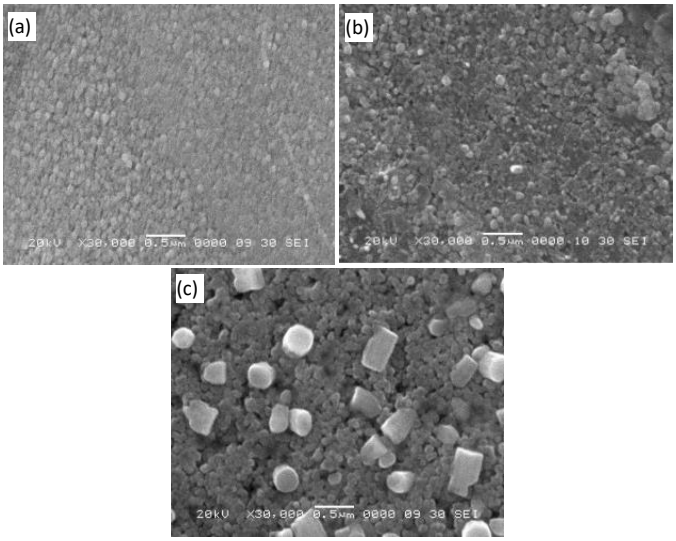

Fig. 5 SEM images of SnO_2-ZnO nanocomposites thin film sample S1, S2 and S3

3.3.2 Transmission Electron Microscope (TEM)

Fig. 6(a) displays the TEM image of the SnO_2-ZnO film (Sample S2) acquired through the scratching of the thin film. The powder was mixed with ethanol. The powder was held in a copper grid. TEM images show that the average grains are nanocrystalline, which means they are less than 8 nm in size and have a shape that is almost spherical. Fig. 6(b) shows the electron diffraction pattern of sample S2. It shows ring patterns that are spotty but continuous, with no extra diffraction spots or rings of secondary phases. This shows that the SnO_2-ZnO nanocomposite films are very crystalline.

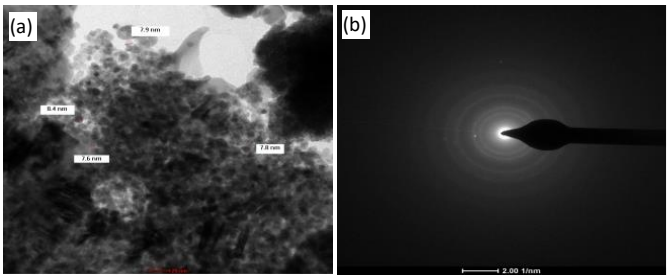

Fig. 6 TEM image (a) and electron diffraction (b) pattern of SnO_2-ZnO film (S2)

3.4 Electrical Characteristics

It has been confirmed that SnO_2-ZnO nanocomposite films were either p-type or n-type semiconductors by measuring the thermoelectric power of the thin film samples. The SnO_2-ZnO nanocomposites films were seen to be the n-type material.

Fig. 7 shows how log(σ) changes with the temperature at which it is used. It is noted that the conductivity of each sample rises as the temperature rises. The rise in conductivity with rising temperature may be due to the negative temperature coefficient of resistance and the semiconducting properties of SnO_2-ZnO nanocomposite films. There are reports [30, 31] that activation energy changes with thickness.

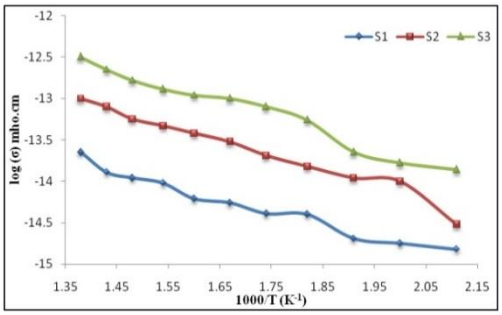

Fig. 7 log(σ) changes with respect to temperature (°C)

The activation energy calculated from the slopes of line for sample S1, S2 and S3. As films thickness goes on increasing, activation energy decreases. The variation of activation energy with thickness is presented in Table 4. The conductivity studies on films show that all the films exhibit two activation energy at different temperature regions. It was shown that as film thickness increases, average grain size from XRD and SEM increases, but activation energy decreases for SnO_2-ZnO nanocomposites films. Conductivity was given by relation,

$$\sigma = \sigma_o \exp(-\Delta E/kT)$$

where, σ = conductivity, σ_o = conductivity constant, k= Boltzmann constant and T= Temperature.

Table 4 Measurement of film thickness grain size and activation energy

Sample	Thickness (nm)	XRD - Average crystalite size (nm)	SEM - Average grain size (nm)	Activation Energy (ΔE) 30 ^{0}C	150 ^{0}C
S1	190	27	29	0.27 eV	0.31 eV
S2	231	31	32	0.23 eV	0.29 eV
S3	362	33	35	0.17 eV	0.21 eV

4. Conclusion

The deposition conditions are ideal for making SnO_2-ZnO nanocomposite films. The structural analysis via XRD indicates the emergence of a mixed phase comprising tetragonal and hexagonal structures. The findings indicates that as the film thickness increases, the texture coefficient and grain size rise, while the values of microstrain, standard deviation, and activation energy decrease. Microstructural characteristics affirm that the synthesised SnO_2-ZnO nanocomposite films exhibited a nanocrystalline structure. The SnO_2-ZnO films' electrical conductivity goes up as the temperature goes up, which shows that they are semiconductors.

Acknowledgements

The authors would like to thank Shri. V.S. Naik, the Principal of Art, Commerce, and Science College in Raver, for letting them use the lab to do this work.

https://doi.org/10.30799/jnst.S105.26110205

Cite this Article as: Pratik H. Naik, Structural, microstructural, and electrical properties of pyrolyzed SnO_2–ZnO nanocomposite thin films, J. Nanosci. Tech. 11(2) (2026) 1058–1061.

References

[1] W. Zhang, W. Zhang, Fabrication of SnO_2-ZnO nanocomposites sensor for selective sensing of try ethylamine and the freshness of fishes, Sens. Actuators B: Chem. 134 (2008) 403-408.

[2] A. Alkaya, R. Kaplan, H. Canbolat, S.S. Hegedus, Nanocomposite ZnO–SnO_2 nanofibers synthesized by electro spinning method, Ren. Ener. 34 (2009) 1595 -1599.

[3] X. Song, Z. Wang, Y. Liu, C. Wang, L. Li, A highly sensitive ethanol sensor based on mesoporous ZnO–SnO_2 nanofibers, Nanotech. 20(2009) 075501.

[4] H. Wang, S. Baek, J. Lee, S. Lim, High photo catalytic activity ZnO-SnO_2 coupled catalysts, J. Chem. Eng. 146 (2009) 355-361.

[5] J. Choi, G. Choi, Electrical and CO gas sensing properties of layered ZnO-CuO sensor, Sens. Actuator. B: Chem. 69 (2000) 120-126.

[6] R.H. Bari, S.B. Patil, A.R. BariI, G.E. Patil, J. Aambekar, Spray pyrolysis nanostructured ZnO thin film sensors for ethanol gas, J. Sens. Transducers 140(5) (2012) 124-132.

[7] N.W. Emanetoglu, C. Gorla, Y. Lu, Epitaxial ZnO piezoelectric thin films for saw filter, Mat. Sci. Semicond. Process. 2(3) (1999) 247-252.

[8] P. Hari, M. Baumer, W.D. Tennyson, L.A. Bumm, ZnO nanorods growth by chemical bath method, J. Non-Cryst. Solid. 354 (2008) 2843-2848.

[9] W.S. Hu, Z.G. Liu, Guo, C. Lin, S.N. Zhu, D. Feng, Preparation of c-axis oriented ZnO optical wave guiding films on fused silica by pulsed laser reactive ablation, Mater. Lett. 25 (1995) 5-8.

[10] L.A. Patil, A.R. Bari, M.D. Shinde, V. Deo, Effect of pyrolysis temperature on structural, microstructural and optical properties of nanocrystalline ZnO powders synthesized by ultrasonic spray pyrolysis technique, J. Experim. Nanosci. 6 (2011) 311-323.

[11] J. Liu, X. Huand, H_2S detection sensing characteristic of CuO/SnO_2 sensor, Sens. 3 (2003) 110-118.

[12] V. Gupta, S. Mozumdar, A. Chowdhuri, K. Sreenivas, Influence of CuO catalyst in the nanoscale rangeon SnO_2 surface for H_2S gas sensing applications, PRAMANA J. Phy. 65 (2005) 647-652.

[13] S. Chappel, A. Zaban, Nano porous SnO_2 electrodes for dye-sensitized solar cells: improved cell performance by the synthesis of 18 nm SnO_2 colloids, Solar Ener. Mater. Solar Cells 71 (2002) 141-152.

[14] G.E. Patil, D.D. Kajale, D.N. Chavan, N.K. Pawar, P.T. Ahire, S.D. Shinde, V.B. Gaikwad, G.H. Jain, Synthesis, characterization and gas sensing performance of SnO_2 thin films prepared by spray pyrolysis, Bull. Mater. Sci. 34 (2011) 1-9.

[15] S. Gnanam, V. Rajendran, Luminance properties of EG- assisted SnO_2 nanoparticles by sol-gel process, Digest J. Nanomat. Biostruc. 5 (2010) 699-704.

[16] C.N. Xu, J. Tamaki, N. Miura, N. Yamazoe, Grain size effects on gas sensitivity of porous SnO_2-based elements, Sens. Actuators B 3 (1991) 147-155.

[17] E. Comini, G. Faglia, G. Sberveglieri, Z. Pan, Z.L. Wang, Stable and highly sensitive gas sensors based on semiconducting oxide nanobelts, Appl. Phys. Lett. 81 (2002) 1869-1871.

[18] Y. Wang, X. Jiang, Y. Xia, A solution-phase, precursor route to polycrystalline SnO_2 nanowires that can be used for gas sensing under ambient concentrations, J. Am. Chem. Soc. 125 (2003) 16176-16177.

[19] A. Chiorino, G. Ghiotti, F. Prinetto, M.C. Carotta, D. Gnani, G. Marinelli, Preparation and characterization of SnO_2 and MO*x*–SnO_2 nanosized powders for thick film gas sensors, Sens. Actuators B 58 (1999) 338-349.

[20] Y. Shimizu, E.D. Bartolomeo, E. Traversa, G. Gusmano, T. Hyodo, K. Wada, M. Egashira, Effect of surface modification on NO_2 sensing properties of SnO_2 varistor-type sensors, Sens. Actuators B 60 (1999) 118-124.

[21] R.H. Bari, S.B. Patil, A.R. Bari, Chemically sprayed SnO_2-ZnO nanocomposites thin films for ethanol gas sensor, J. Nanoeng. Nanomanufactur. 3 (2013) 1-5.

[22] S.D. Sartale, C.D. Lokhande, Preparation and characterization of nickel sulfide thin films deposited by successive ionic Layer adsorption and reaction (SILAR) method, Mat. Chem. Phys. 72 (2001) 101-104.

[23] J.L. Van Heerden, R. Swanepoel, XRD analysis of ZnO thin films prepared by spray pyrolysis, Thin Solid Film. 299 (1997) 72-77.

[24] T. Prasasadu Rao, M.C. Santoshkumar, Effect of thickness on structural, optical and electrical properties of nanostructured ZnO thin films by spray pyrolysis, Appl. Surf. Sci. 255 (2009) 4528-4534.

[25] A.V. Moholkar, S.M. Pawar, K.Y. Rajpuhe, C.H. Bhosale, Effect of concentration of $SnCl_4$ on sprayed fluorine doped tin oxide thin films, J. Alloy. Comp. 455 (2008) 440- 446.

[26] D. Sciti, P. Celotti, G. Pezzotti, S. Guicciardi, Structural model for the binding sites of allosterically potentiating ligands on nicotinic acetylcholine receptors, Appl. Phys. A 86 (2009) 243-249.

[27] S.H. Chaki, M.P. Deshpande, J.P. Tailor, Effect of substrate on CuS/PVA nanocomposite thin films deposited on glass and silicon substrate, Thin Solid Films 550 (2014) 291–297.

[28] G.K. Willamson, W.H. Hall, Measuring crystallite size using X-ray diffraction, J. Chem. Sci. 1953 (2020) 1-4.

[29] B.G. Jeyaprakash, K. Kesavan, R. Ashok Kumar, S. Mohan, A. Amalarani, Temperature dependent grain-size and micro strain of CdO thin films prepared by spray pyrolysis method, Bull. Mater. Sci. 34 (2011) 601-605.

[30] K.C. Sharma, J.C. Garg, Influence of thermal annealing in air on the electro optic characteristic of chemical bath deposited non-stoichiometric cadmium zinc selenide thin films, Phys. D: Appl. Phys. 23 (1990) 1411-1419.

[31] Z.S. EL-Mandouh, M. EL-Shabasy, Transport properties of $(PbTe)_{9.7}Sb_{0.3}$ thin films, FIZIKA A 4 (1995) 17-31.

This article is published as part of the Special Issue *on*

"National Conference on Recent Interdisciplinary Approaches in Allied Sciences, Humanities, Agriculture, Engineering, Law and Management"

Issue Editor:

Dr. B.Y. Bagul

Special Issue Publication and Peer-Review Statement

This article is included in the Special Issue of the journal comprising peer-reviewed papers selected from the National Conference on "Recent Interdisciplinary Approaches in Allied Sciences, Humanities, Agriculture, Engineering, Law, and Management (NCRIASHAELM–2025)", held on 24 December 2025. The conference was sponsored by Pradhan Mantri Uchchatar Shiksha Abhiyan (PM-USHA), Ministry of Education, Government of India, and convened by Dr. B. Y. Bagul, IQAC Coordinator and Head, Department of Physics, Vasantrao Naik Arts, Science and Commerce College. All manuscripts included in this Special Issue underwent editorial screening and peer review in accordance with the journal's standard review policies and ethical guidelines.

https://doi.org/10.30799/jnst.S105.26110205

Cite this Article as: Pratik H. Naik, Structural, microstructural, and electrical properties of pyrolyzed SnO_2–ZnO nanocomposite thin films, J. Nanosci. Tech. 11(2) (2026) 1058–1061.